Turkish Journal of Chemistry

http://journals.tubitak.gov.tr/chem/

Research Article

Turk J Chem
(2020) 44: 1122 – 1133
© TÜBİTAK
doi:10.3906/kim-2003-56

Voltammetric determination of itopride using carbon paste electrode modified with Gd doped TiO_2 nanotubes

Abdulaziz Nabil AMRO[1,*], **Khadijah EMRAN**[1], **Hessah ALANAZI**[2]
[1]Department of Chemistry, College of Science, Taibah University, Madinah, Saudi Arabia
[2]Department of Chemistry, College of Science and Art, Al Jouf University, Qurayyat, Saudi Arabia

Received: 26.03.2020 • **Accepted/Published Online:** 15.06.2020 • **Final Version:** 18.08.2020

Abstract: In the present work TiO_2 nanotubes (TNT) have been synthesized by alkaline hydrothermal transformation. Then they have been doped with Gd element. Characterizations of doped and undoped TNT have been done with TEM and SEM. The chemical composition was analyzed by EDX, Raman and FTIR spectroscopy. The crystal structure was characterized by XRD. Carbon paste electrode has been fabricated and mixed with Gd doped and undoped TNT to form a nanocomposite working electrode. Comparison of bare carbon paste electrode and Gd doped and undoped TNT carbon paste electrode for 1.0×10^{-3} M $K_4[Fe(CN)_6]$ voltammetric analysis; it was observed that Gd doped TNT modified electrode has advantage of high sensitivity. Gd doped TNT modified electrode has been used as working electrode for itopride assay in a pharmaceutical formulation. Cyclic voltammetry analysis showed high correlation coefficient of 0.9973 for itopride (0.04–0.2 mg/mL) with a limit of detection (LOD) and limit of quantitation values (LOQ) of 2.9 and 23.0 µg.mL^{-1} respectively.

Key words: Gd-TiO_2 nanotube, hydrothermal, cyclic voltammetry, itopride, nanocomposite electrode

1. Introduction

Itopride hydrochloride IUPAC name: (N-[4-[2-(dimethyl amino)-ethoxy] benzyl]-3, 4 dimethoxy benzamide hydrochloride) as a benzamide derivative compound is shown in Figure 1. Itopride acts as inhibitor to acetylcholine esterase enzyme, dopamine, and a gastrokinetic effect [1,2]. This pharmaceutical compound is effective for the gastrointestinal symptoms in addition to functional dyspepsia and chronic gastritis [3].

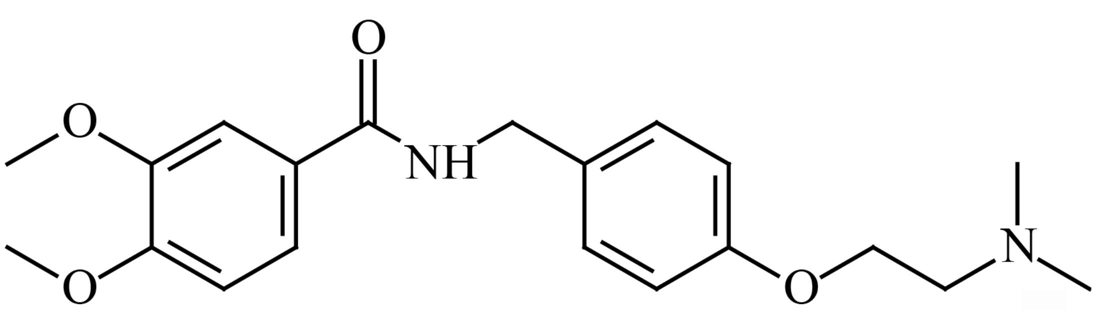

Figure 1. Chemical structure of itopride hydrochloride.

*Correspondence: abdulazizamro@yahoo.com

Most of the studies have used high performance liquid chromatography (HPLC) for itopride assay in pharmaceutical formulation [3–11]. Spectrophotometric methods have also been used for itopride quantitation [12–14]. Pure and combined dosage forms have been analyzed using Potentiometric method [15]. $Ru(bpy)_3^{2+}$ doped silica nanoparticles/chitosan composite films modified electrode has been used as Electrogenerated Chemiluminescence sensor for itopride assay [16]. In recent work Voltammetry has been applied for itopride assay using commercially available platinum electrode [17].

Electrochemical analysis methods have grown in recent years as alternative to other analytical methods [18–20]. Electroanalytical methods have some advantages making them better alternative such as high sensitivity, selectivity, low instrumentation and running cost, easy to handle and short analysis time. Several parameters have played a role in the performance of the electroanalytical methods; one of them is working electrode. Several studies have been done to enhance the performance of working electrodes. In this field carbon paste working electrode achieved a special importance; this importance comes from its simple fabrication steps, in addition to low cost and wide potential window. Various materials such as nanoparticles could be added to carbon paste mixture during preparation to enhance the sensitivity and selectivity of the electrodes [21,22].

Titanium dioxide (TiO_2) is belonging to metal oxide semiconductor that considered as the perfect materials in widespread environmental and medical applications [23–26]. TiO_2-based nanomaterials as nanotubes have been intensively studied and widely used due to their excellent electrolytic and electrolysis performance, high chemical stability and efficiency, nontoxicity and low cost [27–30]. The high cation exchange capacity on titanium dioxide nanotubes (TNT) provides the possibility of achieving a high loading of active compound on it, which makes it one on the best sensor. Otherwise, the high specific surface area and absence of micropores in TNT which facilitate transport of reagent the active sites. The bandwidth between the valence and conduction bands limits its activity [31]. By addressing this issue, doping with elements as rare-earth that have a large atomic number have been devoted [32–35]. The electronic energy levels in rare-earth elements are rich and improve its photocatalytic and electrocatalytic activity.

In this study, TiO_2 nanotubes have been prepared then doped with Gd, after the characterization Gd doped TiO_2 nanotubes. Carbon paste electrode has been mixed with different doses of TiO_2 nanotubes and Gd doped TiO_2 nanotubes, cyclic voltammetry has been established to study the performance of each fabricated electrode, then the electrode exhibited the best performance that has been used in voltammetric analysis of itopride in a pharmaceutical formulation.

2. Experimental

2.1. Materials and reagents

The standard pharmaceutical formulation of itopride hydrochloride was obtained from Trium pharma (Jordan), sodium sulphate anhydrous Na_2SO_4 from Janssen Chemica. The supporting electrolyte 1.0 M Na_2SO_4 was prepared using Milli-Q water. 1.0 M Na_2SO_4 supporting electrolyte was used for the preparation of stock solutions and standard working solutions. $K_4Fe(CN)_6.3H_2O$ was obtained from (Sigma Aldrich), Graphite powder from (BDH), and Paraffin liquid light BP from (Pacegrove).

2.2. Synthesis of TNTs

The method of preparation of TNT and doped Gd-TNT was based on alkaline hydrothermal transformation. A weighted amount of TiO_2 powder [P25, (99.5%, 21 nm), Sigma-Aldrich, USA] was added to 30 mL of 10 mol dm^{-3} potassium hydroxide [KOH,Sigma-Aldrich, USA] solution. After stirring for 30 min and the mixture was transferred into a Teflon-lined stainless-steel autoclave and was heated for 24 h at 150 °C. The white Powderly precipitate was thoroughly washed with deionized water then with dilute HCl until the pH of washing solution reached 6.5 then with deionized water again, followed by drying for 10 h at 90 °C, and calcinating at 400 °C for 2 h. Gd-TNT was synthesized by adding $Gd(NO_3)_3$ to the TiO_2 in the KOH solution followed by the hydrothermal and postsynthetic treatments as described above for the undoped TNTs [35].

2.3. Characterizations

The morphology of undoped TNTs and doped Gd-TNTs was examined by Transmission Electron Microscope (TEM, JEOL JEM 1400, Japan) and scanning electron microscopy equipped (SEM, Superscan SS-550, Shimadzu, Japan). The chemical composition was analyzed by energy dispersive X-ray analysis equipped (EDX, Superscan SS-550, Shimadzu, Japan). The crystal structure of the as-prepared sensors were characterized by a X-ray diffraction (XRD, Shimadzu, XRD-7000, Japan) at 40 kV and 30 mA, using CuK$_\alpha$ incident beam (λ = 0.154nm). Raman spectroscopy was performed on a Raman microscope (Raman, Sentrarra, Bruker, USA) from 50 cm^{-1} to 1200 cm^{-1}. Infrared (FT-IR) absorption spectra of the KCl disks containing powder samples were recorded on a Thermo IS-10 instrument FT-IR spectrometer (Thermo Fisher Scientific Inc., Madison, WI, USA) at a resolution of 4 cm^{-1} in the range of 400–4000 cm^{-1}.

2.4. Modified carbon paste electrode fabrication

For fabrication of carbon paste modified electrodes, graphite powder, TNT, and Gd-TNT have been mixed as in the Table 1.

Table 1. Quantities of fabricated electrodes contents.

Electrode code	Graphite powder (mg)	TNT(mg)	Gd-TNT(mg)
C paste	200	0	0
F1	200	25	0
F2	200	50	0
G1	200	0	25
G2	200	0	50

After that mixture powder was dispersed in 1.0 mL dimethyl formamide (DMF) then homogenized for 20 min in ultrasonic bath. After that DMF was vaporized from the mixture using oven at 80 °C overnight. Dry mixture was mixed with 100 µL paraffin oil using spatula. Micropipette tip of 2 mm end was filled with mixture paste. For electrical connection copper wire connection was made passed through the edge of the tip.

2.5. Voltammetric analysis apparatus

Potentiostat (Metrohm Autolab) PGSTAT 204 was used for voltammetric measurements. All measurements were carried out using a 3 electrodes system; where Ag/AgCl (3 M KCl) was used as reference electrode, platinum (Pt) sheet as counter electrode, and fabricated carbon paste as working electrode.

3. Results and discussion

3.1. Morphology and structure analysis

Synthesized TNTs and Gd-TNTs have uniform and hollow multiwall structure, Figures 2a and 2b. The tubular structures of TNT have an outer diameter around 6.5 to 10.6 nm, the length of about 51 nm and Gd-TNTs are in the range 6.1 nm–14.2 nm diameter of range. This is agreed with SEM images in Figures 2c and 2d. where the samples are aggregate as thread network. EDX analysis, Figures 2e and 2f, shows uniform distributions of about 2.92% of Gd in Gd-TNTs.

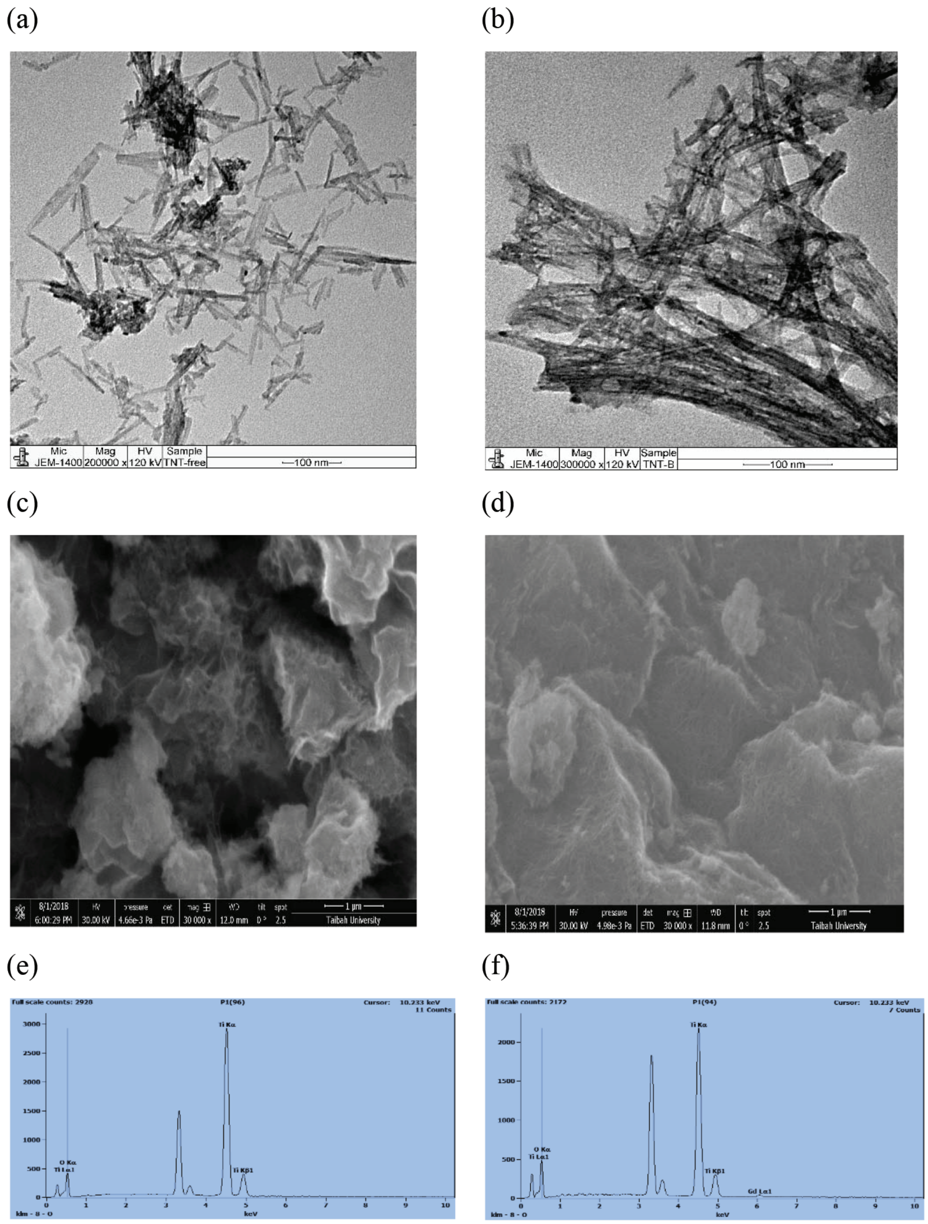

Figure 2. TEM images of (a) undoped TNTs; (b) Gd –TNTs , SEM images of (c) undoped TNTs(d); Gd –TNTs and EDX of undoped TNTs (e); Gd-TNTs (f).

The crystal phase of TNTs and Gd-TNTs was identified by XRD. Diffraction peaks of TNT on Figure 3a observed at 24.90°, 48.10°, 55.91°, are diffractions of (1 0 1), (2 0 0) and (2 1 1) crystal planes of anatase TiO_2, respectively (JCPDS, card no.: (00-021-1272). Meanwhile there are characteristic peaks of Gd observed at 29.28°, 31.64°, 47.89°, and 58.72°assigned to (2 0 1), (0 4 0), (3 4 1), and (6 1 1), respectively [35], owes to Gd ion as Gd_2TiO_5 (JCPDS, card no.: (00-021-0342).

Figure 3b shows the same strong peaks of Raman spectra obtain of synthesized sensors. The peaks observed at around 143 cm^{-1} (E_{1g}), 198 cm^{-1} (E_{2g}), 394 cm^{-1} (B_{1g}), and 638 cm^{-1} (E_{3g}), respectively, were attributed to anatase TiO_2 which agree with previous studies [35, 36] and reveal the characteristics of the anatase phase of the sensors. This result is also an evidence to verify that Gd introduced into the lattice or interstitial site of TiO_2.

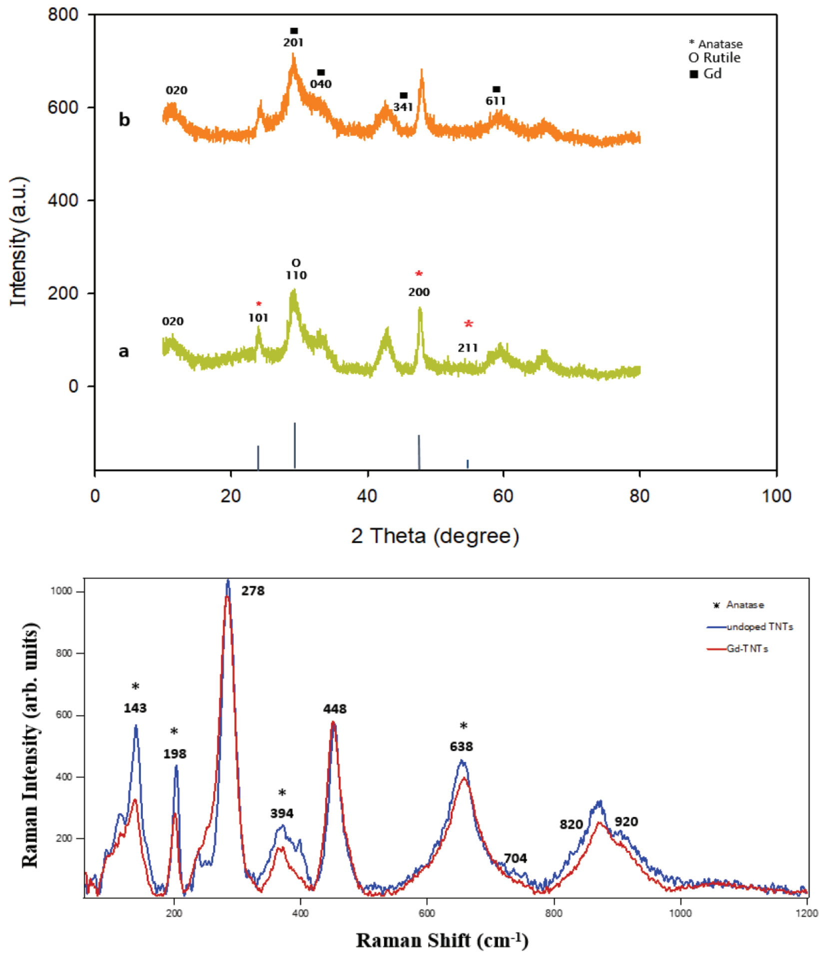

Figure 3. XRD patterns (a) and Raman spectrum (b) of TNT and Gd-TNTs.

The band at 278 cm^{-1} was assigned to the stretching vibration of Ti-O-K bonds and the bands at 198 cm^{-1} and 394 cm^{-1} corresponded to anatase Ti-O-Ti [35,37]. The band at 448 cm^{-1} was related to Ti-O-Ti crystal phonons [38]. The bands at 704 cm^{-1} and 820 cm^{-1} corresponded to covalent Ti-O-H bonds [39], and the band at 920 cm^{-1} was assigned to surface Ti-O-K vibrations [35]

3.2. FTIR analysis

IR spectra of TNT (a) and Gd-TNT (b) are depicted in Figure 4. Both spectra display the broad band at around at 3432.53 cm^{-1}, corresponding to the surface adsorbed water and hydroxyl groups in tubular structure sensors. The large amount of hydroxyl groups on sensors wall enhance their performance for the photo excited electrons capture and profiled the holes to produce the reactive oxygen species in the photocatalytic [40]. The bands at 1627.87 cm^{-1} and 955.87 cm^{-1} can be attributed to the H-O-H bending vibration of the adsorbed water. For synthesized sensor, another typical band at around 446±4 cm^{-1} is originated from the Ti-O-Ti band of TNT and to the asymmetric of Gd-Ti-O in doped Gd-TNT [41].

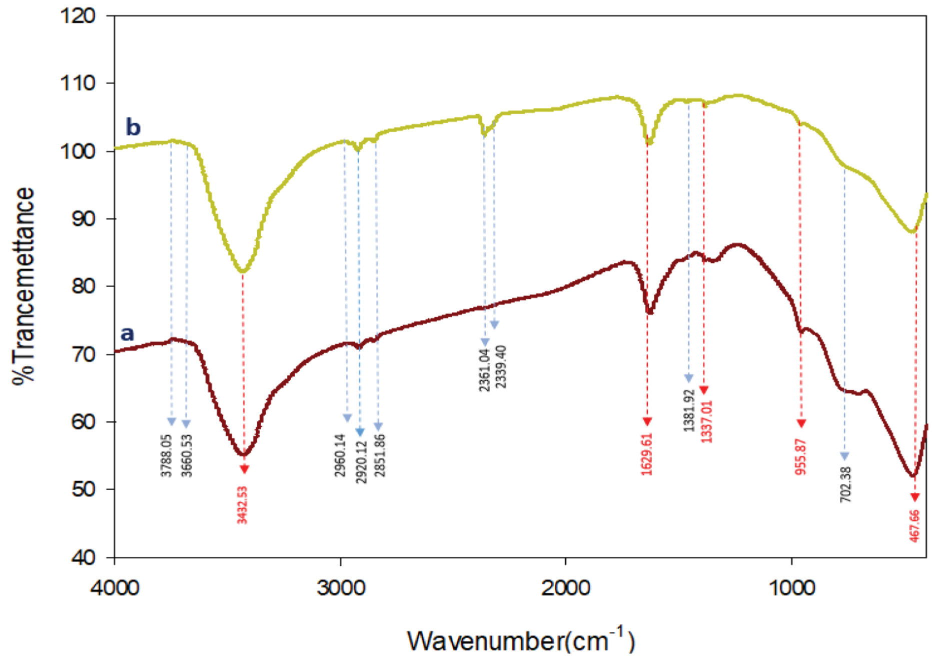

Figure 4. Infrared spectrum of TNTs (a); Gd–TNTs (b).

3.3. Electrochemical performance of fabricated electrodes

Cyclic voltammetry was carried out to study the electrochemical performance of fabricated electrodes. Figure 5 shows voltammograms of 1.0×10^{-3} M $K_4[Fe(CN)_6]$ with fabricated working electrodes. It could be concluded that doping TiO_2 with Gd enhances both anodic and cathodic peak currents, where G2 electrode anodic peak current reaches 56 µA compared to 31 µA for bare C paste electrode. Furthermore, G2 cathodic peak current reaches 52 µA which is the highest compared to other studied electrodes. According to the voltammograms of G1 and G2 of Figure 5, it can be concluded that increasing Gd-TNT portion in the fabricated electrodes has a positive impact on electrode sensitivity.

A comparison has been established between fabricated working electrodes for itopride pharmaceutical formulation assay. The voltammograms in Figure 6 show significant difference in performance between studied working electrodes. Figure 6 shows drastic increase in the anodic peak current of G2 working electrode for itopride compared to G1, bare C paste, and (F) electrodes.

When G2 was used as working electrode it showed ΔE_p of 1.1 V; where ($\Delta E_p = E_{pa} - E_{pc}$), which is greater than the value of 59/n mV expected for a reversible system [42] suggesting that itopride with G2 working electrode has irreversible behavior in aqueous medium.

3.4. Influence of scan rate (υ):

Itopride oxidation mechanism was investigated by study the effect of scan rate on the electrode response. Applied scan rate is ranging from 40 to 180 mV/s. Results are summarized in Figure 7, which indicated that as scan rate increases, anodic peak current increases (Figures 7a and 7b), furthermore it shifts the anodic peak

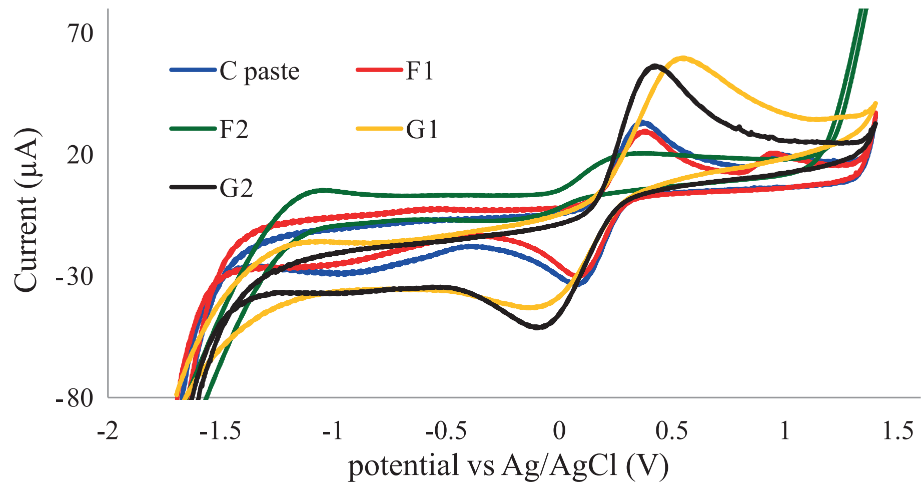

Figure 5. Cyclic voltammograms of 1.0×10^{-3} M $K_4[Fe(CN)_6]$, CPE scan rate .0.1V S^{-1}.

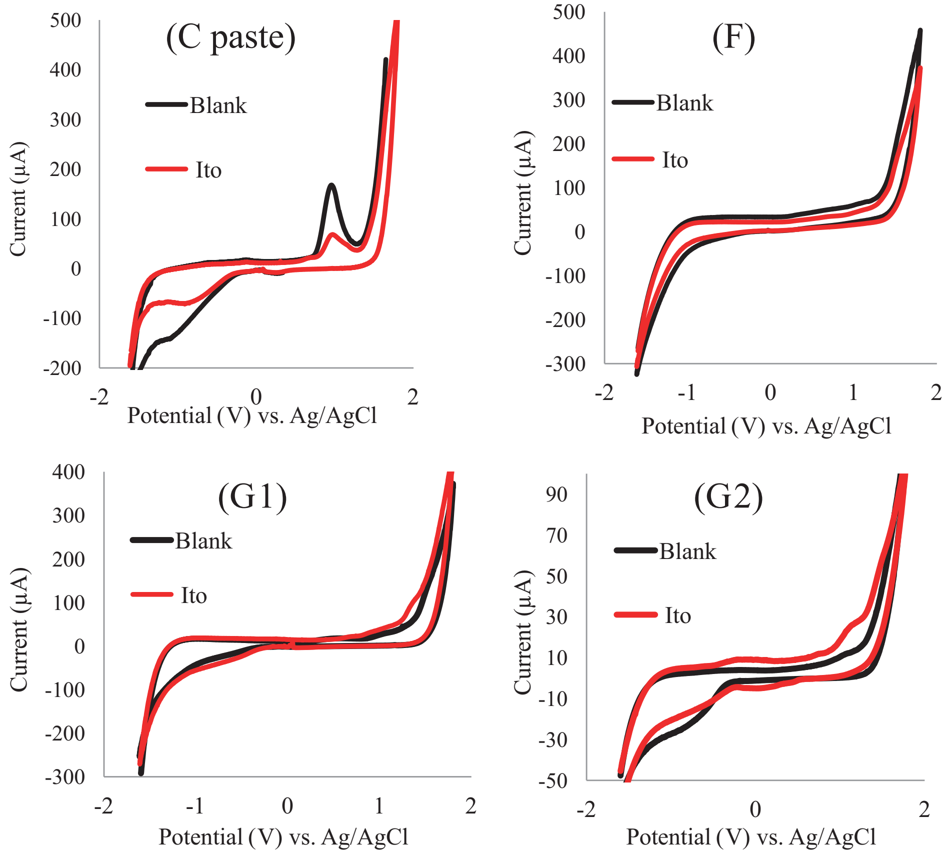

Figure 6. CV Comparison between working electrodes (pure carbon paste, F, G1, and G2) for 0.20 mg/mL itopride assay in 1 M Na_2SO_4 supporting electrolyte and 1M Na_2SO_4 (blank), scan rate 0.1V S^{-1}.

potential (Epa) positively (Figure 7a), which interprets the irreversibility of the electrode process. Figure 7c shows log (ip) vs. log (υ) plot which verified linear relationship with slope 0.693, slope value is closer to 0.5, the theoretical value indicated redox process controlled typically by diffusion mass transport only, rather than 1.0 value which typically indicated redox processes controlled by adsorption [42,43].

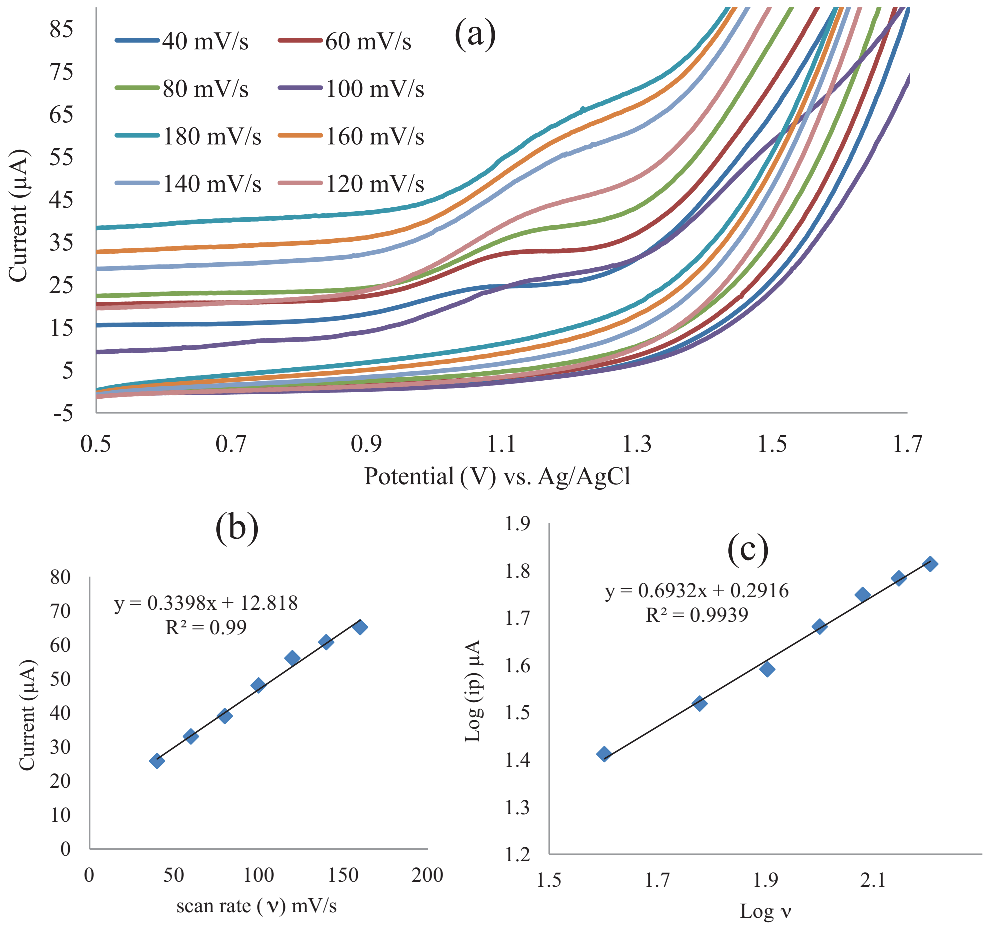

Figure 7. (a) Effect of scan rate on the CVs of 0.20 mg/mL itopride in 1M Na_2SO_4 supporting electrolyte, G2 working electrodes, in the range of 40–180 mV/s; (b) Plot of ip vs. ? (c) Plot of log I vs. log ?.

3.5. Analytical performance

To evaluate the performance of fabricated sensor (G2), a calibration curve was established in the acquired optimum conditions for itopride assay in a pharmaceutical formulation. Figure 8 shows cyclic voltammograms of itopride in a pharmaceutical formulation (0.04–0.2 mg/mL). Standard calibration curve illustrates high correlation (R^2= 0.9973) in addition to high sensitivity. Each concentration has been done triplicate with relative standard deviation (RSD) of all concentrations less than 1%. Limit of detection (LOD) and limit of quantitation values (LOQ) found to be 2.9 and 23.0 µg.mL^{-1}, respectively. Where LOD and LOQ of itopride were determined based on signal-to-noise ratio of 3 and 10, respectively.

Table 2 shows a comparison between present work and other methods used for itopride determination. This comparison includes precession and LOD. Data in Table 2 indicate that CV analysis of itopride using Gd-TNT electrode has a comparable LOD and precession with chromatographic and spectroscopic methods.

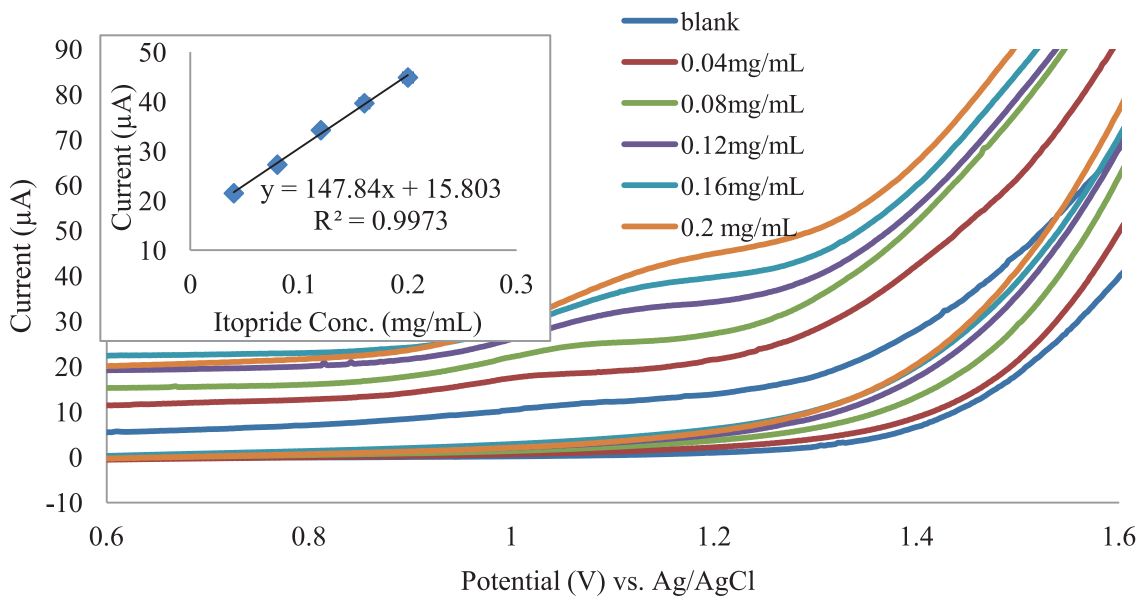

Figure 8. CV study of itopride (0.04–0.20 mg/mL), G2 working electrode, Na_2SO_4 (1 M) supporting electrolyte, scan rate $0.1 V.s^{-1}$, each concentration has been done triplicate.

Table 2. Comparison in LOD and precession between present study and other methods used for itopride determination.

Method	LOD	Precession	Reference
RP-HPLC fluorescence detection	5 ng/mL	2.81%	9
RP-HPLC/UV detection	12 ng/mL	0.87%	4
Potentiometric	3.98 µM	0.658%	15
UV Spectroscopy	0.5–1.5 µg/mL	0.05%	12
UV–visible spectroscopy	-	1.48%	13
CV-GC electrode	3.50 µg/mL	1.02%	17
CV-C paste Gd-TNT electrode	2.90 µg/mL	0.82%	Present work

4. Conclusions

In the present work, TiO_2 nanotubes have been synthesized and doped with Gd element, and then it has been fully characterized. A composite of carbon paste modified with Gd doped TiO_2 nanotubes electrode have shown higher sensitivity compared to bare and undoped TiO_2 nanotubes carbon paste electrode. When Gd doped TiO_2 nanotubes electrode has been applied for cyclic voltammetry of itopride in a pharmaceutical formulation, it has shown high performance compared to commercially available electrode.

References

1. Kim YS, Kim TH, Choi CS, Shon YW, Kim SW et al. Effect of itopride, a new prokinetic, in patients with mild GERD: a pilot study. World Journal of Gastroenterology 2005; 11: 210-214. doi: 10.3748/wjg.v11.i27.4210

2. Katagiri F, Shiga T, Inoue S, Sato Y, Itoh H et al. Effects of itopride hydrochloride on plasma gut-regulatory peptide and stress-related hormone levels in healthy human subjects. Pharmacology 2006; 77:115- 121. doi: 10.1159/000093485

3. Ma J, Yuan LH, Ding MJ, Zhang J, Zhang Q et al. Determination of itopride hydrochloride in human plasma by RP-HPLC with fluorescence detection and its use in bioequivalence study. Pharmaceutical Research 2009; 59: 189-193. doi: 10.1016/j.phrs.2008.11.007

4. Khan A, Iqbal Z, Khadra I, Ahmad L, Khan A et al. Simultaneous determination of domperidone and Itopride in pharmaceuticals and human plasma using RP-HPLC/UV detection: Method development, validation and application of the method in in-vivo evaluation of fast dispersible tablets. Journal of Pharmaceutical and Biomedical Analysis 2016; 121: 6-12. doi:10.1016/j.jpba.2015.12.036

5. Harun Rasheed S, Ramakotaiah M, Ravi Kumar K, Nagabhushanam CH, Prasada CHMM. Estimation of Rabeprazole Sodium and Itopride Hydrochloride in Tablet Dosage Form Using Reverse Phase High Performance Liquid Chromatography. E – Journal of Chemistry 2011; 8(1): 37-42. doi: 10.1155/2011/683845

6. Pillai S, Singhvi I. Quantitative Estimation of Itopride Hydrochloride and Rabeprazole Sodium from Capsule Formulation. Indian Journal of Pharmaceutical Science 2008; 70 (5): 658-661. doi: 10.4103/0250-474X.45411

7. Thiruvengada Rajan VS, Mohamed Saleem TS, Ramkanth S, Alagusundaram M, Ganaprakash K et al. A Simple RP-HPLC Method for Quantitation of Itopride HCl in Tablet Dosage Form. Journal of Young Pharmacists 2010; 2(4): 410-413. doi: 10.4103/0975-1483.71634

8. Suganthi A, John S, Ravi TK. Simultaneous HPTLC Determination of Rabeprazole and Itopride Hydrochloride from Their Combined Dosage Form. Journal of Pharmaceutical Science 2010; 70 (3): 366-368. doi: 10.4103/0250-474X.43004

9. Sun Y, Zhang Z, Xi Z, Shi Z, Tian W. Determination of itopride hydrochloride by high-performance liquid chromatography with Ru(bpy)3^{2+} electrogenerated chemiluminescence detection. Analytica Chimica Acta 2009; 648:174-177. doi: 10.1016/j.aca.2009.07.003

10. Gupta KR, Chawla RB, Wadodkar SG. Stability indicating RP-HPLC method for simultaneous determination of pantoprazole sodium and itopride hydrochloride in bulk and capsule. Orbital Electronic Journal of Chemistry, Campo Grande 2010; *2*(3): 209-224. doi: 10.17807/orbital.v2i3.87

11. Lee HW, Seo JH, Choi SK, Lee KT. Determination of itopride in human plasma by liquid chromatography coupled to tandem mass spectrometric detection: Application to a bioequivalence study. Analytica Chimica Acta 2007; 583: 118-123. doi: 10.1016/j.aca.2006.09.061

12. Gupta KR, Joshi RR, Chawla RB, Wadodkar SG. UV Spectrophotometric Method for the Estimation of Itopride Hydrochloride in Pharmaceutical Formulation E-Journal of Chemistry 2010; 7: S49-S54. doi: 10.1155/2010/526891

13. Ramadan NK, El-Ragehy NA, Ragab M, TEl-Zeany BA. Simultaneous determination of a binary mixture of pantoprazole sodium and itopride hydrochloride by four spectrophotometric methods. Spectrochimica Acta A: Molecular and Biomolecular Spectroscopy 2015; 137: 463-470. doi.org/10.1016/j.saa.2014.09.003

14. Sabnis SS, Dhavale ND, Jadhav VY, Gandhi SV. Spectrophotometric simultaneous determination of Rabeprazole Sodium and Itopride Hydrochloride in capsule dosage form. Spectrochimica Acta A: Molecular and Biomolecular Spectroscopy 2008; 69: 849-852. doi.org/10.1016/j.saa.2007.05.048

15. Ragab MT, Abd El-Rahman MK, Ramadan NK, El-Ragehy AN, El-Zeany B. A Novel potentiometric application for the determination of pantoprazole sodium and itopride hydrochloride in their pure and combined dosage form. Talanta 2015; 138: 28-35. doi: 10.1016/j.talanta.2015.01.045

16. Hun X, Zhang Z. Electrogenerated chemiluminescence sensor for itopride with $Ru(bpy)_3^{2+}$ doped silica nanoparticles/chitosan composite films modified electrode. Sensors and Actuators B 2008; 131: 403-410. doi.org/10.1016/j.snb.2007.11.055

17. Amro AN. Voltammetric Method Development for Itopride Assay in a Pharmaceutical Formulation. Current Pharmaceutical Analysis 2020; 16(3) 312-318. doi: 10.2174/1573412915666190912122421

18. Siddique MR, Alothman ZA, Rahman N. Analytical techniques in pharmaceutical analysis: A review. Arabian Journal of Chemistry 2017; 10: s1409-s14021. doi: 10.1016/j.arabjc.2013.04.016
19. Gupta VK, Rajeev J, Keisham R, Nimisha J, Shilpi A. Voltammetric techniques for the assay of pharmaceuticals-a review. Analytical Biochemistry 2011; 408: 179-196. doi: 10.1016/j.ab.2010.09.027
20. Fedder M, Amro A, Bin Oun S. Voltammetric Determination of vildagliptin in a pharmaceutical formulation. Tropical Journal of Pharmaceutical Research 2018; 17 (9): 1847-1852. doi; 10.4314/tjpr.v17i9.24
21. Ianesko F, de Lima CA, Antoniazzi C, Santana ER, Piovesan JV et al. Simultaneous Electrochemical Determination of Hydroquinone and Bisphenol A using a Carbon Paste Electrode Modified with Silver Nanoparticles. Electroanalysis 2018; 30: 1946-1955. doi: 10.1002/elan.201800074
22. Pourghobadi R, Baezzat MR. Alumina nanoparticles modified carbon paste electrode as a new voltammetric sensor for determination of dopamine. Iranian Chemical Communication 2018; 6 (4): 359-368. doi: 10.30473/ICC.2018.4143
23. Roy P, Berger S, Schmuki P. TiO_2 nanotubes: synthesis and applications. Angewandte Chemie International Edition 2011; 50 (13): 2904-2939. doi: 10.1002/anie.201001374
24. Huang S, Si Z, Li X, Zou J, Yao Y et al. A novel Au/r-GO/TNTs electrode for H_2O_2, O_2 and nitrite detection. Sensors Actuators B Chemical 2016; 234: 264-272. doi: 10.1016/j.snb.2016.04.167
25. Wang Q, Huang JY, Li HQ, Zhao AZJ, Wang Y et al. Recent advances on smart TiO2 nanotube platforms for sustainable drug delivery applications. International Journal of Nanomedicine 2017; 12: 151-165. doi: 10.2147/IJN.S117498
26. Emran KM, Ali SM, Alanazi HE. Novel Hydrazine Sensors based on Pd Electrodeposited on Highly Dispersed Lanthanide -doped Ti2 Nanotubes. Journal of Electroanalytical Chemistry 2020; 856: 113661-113668. doi: 10.1016/j.jelechem.2019.113661
27. Beydoun D, Amal R, Low G, McEvoy S. Role of nanoparticles in photocatalysis. Journal of Nanoparticles Research 1999; 1: 439-458. doi:10.1023/A:1010044830871
28. Wang X, Li X, Liu D, Song S, Zhang H. Green synthesis of Pt/CeO_2/graphene hybrid nanomaterials with remarkably enhanced electrocatalytic properties. Chemical Communications 2012; 48: 2885-2887. doi:10.1039/C2CC17409J
29. Wang W, Li G, Xia D, An T, Zhao H et al. Photocatalytic nanomaterials for solar-driven bacterial inactivation: recent progress and challenges. Environmental Science: Nano 2017; 4: 782-799. doi:10.1039/C7EN00063D
30. Clarizia L, Russo D, Di Somma I, Andreozzi R, Marotta R. Metal-based semiconductor nanomaterials for photocatalysis. Multifunctional Photocatalytic Materials for Energy. Elsevier 2018: 187-213.
31. Li ZX, Shi FB, Zhang T, Wu HS, Sun LD et al. Stabilized ordered meso porous titania for near-infrared photocatalysis. Chemical Communications 2011; 47: 8109-8111. doi: 10.1039/C1CC12539G
32. Wang J, Zhou Y, Xiong B, Zhao Y, Huang X et al. Fast lithium-ion insertion of TiO2 nanotube and graphene composites. Electrochimica Acta 2013; 88: 847-857. doi: 10.1016/j.electacta.2012.10.010
33. Reszczyńska J, Grzyb T, Sobczak JW, Lisowski W, Gazda M et al. Lanthanide co-doped TiO_2: the effect of metal type and amount on surface properties and photocatalytic activity. Applied Surface Science 2014; 307: 333-345. doi: 10.1016/j.apsusc.2014.03.199
34. Parnicka P, Mazierski P, Lisowski W, Klimczuk T, Nadolna J et al. A new simple approach to prepare rare-earth metals-modified TiO_2 nanotube arrays photoactive under visible light: surface properties and mechanism investigation. Results in Physics 2018; 12: 412-423. doi:10.1016/j.rinp.2018.11.073
35. Emran KM., Hessah E. Alanazi. Fabrication and Characterization of Lanthanide-TiO2 Nanotube Composites, 2020.
36. Huang S, Si Z, Li X, Zou J, Yao Y et al. A novel Au/r-GO/TNTs electrode for H_2O_2, O_2 and nitrite detection. Sensors Actuators B Chemistry 2016; 234: 264-272. doi: 10.1016/j.snb.2016.04.167

37. Ali I, Kim J-O. Visible-light-assisted photocatalytic activity of bismuth-TiO_2 nanotube composites for chromium reduction and dye degradation. Chemosphere 2018; 207: 285-292. doi: 10.1016/j.chemosphere.2018.05.075

38. Bavykin DV, Friedrich JM, Walsh FC. Protonated titanates and TiO2 nanostructured materials: synthesis, properties, and applications. Advanced Materials, 2006; 18 (21): 2807-2824. doi:10.1002/adma.200502696

39. Turki A, Kochkar H, Guillard C, Berhault G, Ghorbel A. Effect of Na content and thermal treatment of titanate nanotubes on the photocatalytic degradation of formic acid Applied Catalysis B: Environmental 2013;138: 401-415.

40. Zhao F, Rong Y, Wan J, Hu Z, Peng Z et al. High photocatalytic performance of carbon quantum dots/TNTs composites for enhanced photogenerated charges separation under visible light. Catalysis Today 2018; 315: 162-170. doi: 10.1016/j.cattod.2018.02.019

41. Nie J, Mo Y, Zheng B, Yuan H, Xiao D. Electrochemical fabrication of lanthanum-doped TiO_2 nanotube array electrode and investigation of its photoelectrochemical capability. Electrochimica Acta 2013; 90: 589-596. doi: 10.1016/j.electacta.2012.12.049

42. Bard AJ, Faulkner LR. Electrochemical Methods: Fundamentals and Applications. 2nd edition. New York, NY, USA: Wiley, 2001.

43. Khalifa A, El-Desoky H, Abdel-Galeil M. Graphene-based sensor for voltammetric quantification of dapoxetine hydrochloride: a drug for premature ejaculation in formulation and human plasma. Journal of the Electrochemical Society 2018; 165 (3): H128-H140.